On the Use of the Atomic Force Microscope To Monitor Physical Degradation Of Polymeric Coating Surfaces

Mark R. VanLandingham, Tinh Nguyen, W. Eric Byrd, and Jonathan W. Martin—
National Institute of Standards and Technology*

The atomic force microscope (AFM) was used to monitor changes in surface features of an acrylic melamine coating that was exposed to a variety of conditions. Exposure to ultraviolet (UV) radiation and high relative humidity caused general roughening of the surface and the formation of pits. Further, the damage of the coating surface was much more substantial for exposure to high relative humidity compared to exposure to dry environments. This difference in degradation rates correlated with measurements of chemical degradation determined using infrared spectra that were acquired along with the AFM images.

INTRODUCTION

Predicting the service life of an engineering material requires relating laboratory and field exposure testing. Such relationships are difficult to establish because of the aperiodic behavior and unpredictable changes in trend lines associated with the various weather elements.[1,2] Hence, laboratory experiments should not be expected to simulate outdoor exposure conditions, but rather should cover the range of expected field exposure conditions in a well-monitored and well-controlled fashion. Service life is generally defined as the time after installation at which an unacceptable percent of a product population fails during service exposure and operation. Because this percentage is commonly much less than one percent, the factors affecting a product's early times-to-failure are of particular interest. Thus, isolating factors and determining mechanisms that cause these early failure events become primary objectives for any service life prediction methodology.[3]

The research reported in this paper is part of an ongoing effort in service life prediction of polymeric coating materials. Previous research of polymer coating degradation has been focused primarily on the chemical degradation mechanisms.[4-6] For example, Bauer et al.[4-6] studied the degradation of acrylic melamine coatings using Fourier transform infrared (FTIR) spectroscopy. In a few studies, mechanical property changes of coatings have been investigated,[7-10] in which changes in glass transition temperature, crosslink density, and fracture toughness have been reported. Further, while appearance-related measurements, such as gloss, are often used as a measure of physical degradation, the actual changes in surface topography (e.g., roughness changes, the formation of surface defects, etc.) that affect these measurements have not been studied extensively. In cases where surface topographical changes have been quantified, the focus has been on relatively large-scale changes affecting appearance,[11] while little research has focused on the early stages of physical degradation that occur on a submicrometer length scale. As a consequence, relationships between physical and chemical degradation are lacking.

Because two main functions of a polymer coating are to enhance appearance and to reduce or eliminate corrosion, early failure events are more likely to be associated with physical changes in the coating surface rather than changes in coating chemistry. In this service life prediction research, chemical changes in an acrylic melamine coating are studied using FTIR spectroscopy, while atomic force microscopy (AFM) is used to study early stages of physical degradation. The individual and combined effects of exposure to spectral ultraviolet (UV) radiation, temperature, and relative humidity (RH) are investigated systematically using well-controlled and well-monitored laboratory exposure conditions, as described in the Experimental section. To build on previous literature, an unpigmented acrylic melamine was chosen as a model polymeric coating (see Experimental section). The results of the AFM studies of physical degradation are then presented, and the relationships between chemical and physical degradation are discussed, particularly with regard to possible degradation mechanisms.

*Building Materials Division, 100 Bureau Dr., Stop 8621, Gaithersburg, MD 20899-8621.

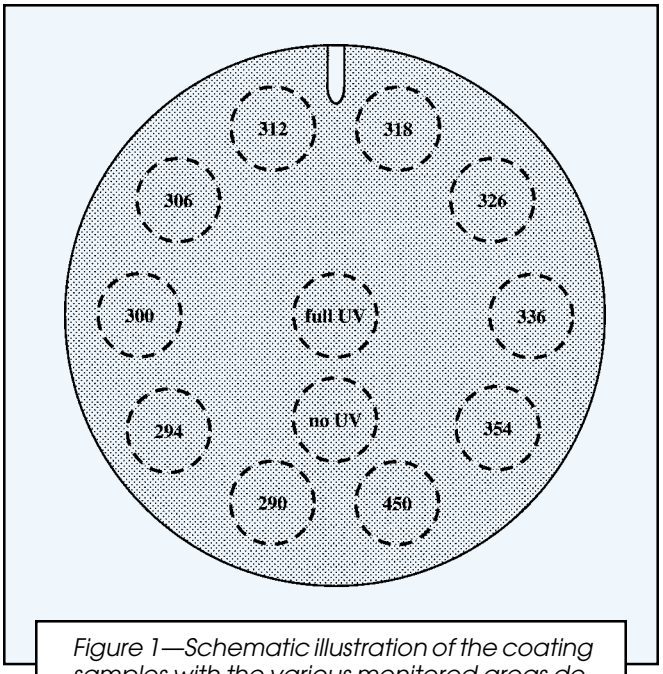

Figure 1—Schematic illustration of the coating samples with the various monitored areas denoted by the dashed circles and identified by the corresponding UV exposure conditions.

EXPERIMENTAL*

Solar Simulators and Exposure Cells

The solar simulators and exposure cells have been described in detail elsewhere.[3] Essentially, two solar simulators (Oriel) were used as the source of the UV radiation, and each solar simulator illuminated a set of four exposure cells that were placed in the sample chamber directly below the light sources. Each solar simulator was equipped with a 1000 W xenon arc lamp and an optical system that removed the visible and infrared portions of the xenon arc radiant flux and then homogenized and collimated the beam. The removal of the visible and infrared portions greatly reduced the amount of thermal radiant energy in the beam so that the corresponding increase in temperature within the specimen exposure cells was less than 2°C above the ambient temperature (see the following secton on Materials for information regarding cell temperatures). Collimation of the light beam was estimated to be within ± 1°.† The radiant flux from each light source was regulated continuously during the experiments using feedback between a light intensity controller that regulated electrical current density supplied to the lamp and a fiber optic cable that monitored the radiant flux of the lamp.

Each exposure cell was designed to simultaneously expose a sample to 11 well-defined spectral radiation bandwidths at the same temperature and relative humidity. Further, the exposure environment within each exposure cell in a set could be the same or different from that of the other exposure cells. The most important aspects of the exposure cells included the tight design tolerances, the window construction, and the use of interference filters for the windows. The tight tolerances allowed for an essentially leak-proof chamber into which air of a specified temperature and relative humidity was pumped through inlet and outlet ports. A thermocouple within the cell was used to monitor temperature. The relative humidity of the flowing air was monitored by rerouting a portion of the air through a chilled mirror hygrometer for five minutes out of every 20 minutes over the duration of an experiment. A four-layered construction was used for the cells, as described in detail elsewhere.[3] Each layer had 11 windows machined into an aluminum plate, one window in the center of each plate and the other 10 windows along the perimeter of each plate. In each of the 10 perimeter windows, a narrow bandwidth interference filter was inserted to allow different areas of the coatings to be exposed to different UV wavelengths (see *Figure* 1). The transmittance spectra for the filters were fully characterized.[3] The nominal center wavelengths for these filters were 290, 300, 306, 312, 318, 326, 336, 354, and 450 nm. Note that 290 nm is the lowest wavelength of solar radiation reaching the Earth's surface.[12] The filter thicknesses were selected so that the coating regions underneath the different filters degraded at similar rates.[3] The center window transmitted all the spectral radiant energy emitted by the solar simulators. A twelfth window was located in the bottom two plates only, i.e., without a corresponding set of windows in the upper two plates, such that this region of the sample received no UV radiation but was exposed to the controlled temperature and relative humidity of the cell environment.

Materials

The coating system selected was a model thermosetting acrylic melamine polymeric system that was similar to systems widely used as automotive clearcoats. This system was chosen because analogues of this coating are used in a variety of coating applications[4,13] and the degra-

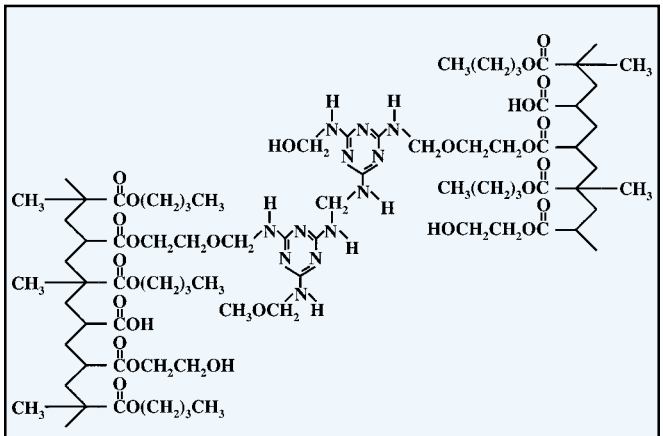

Figure 2—Crosslinked structure of the acrylic melamine coating as determined from FTIR spectroscopy results.

*Certain commercial instruments and materials are identified in this paper to adequately describe the experimental procedure. In no case does such identification imply recommendation or endorsement by the National Institute of Standards and Technology, nor does it imply that the instruments or materials are necessarily the best available for the purpose.

†Throughout this text, each number following the symbol ± is the numerical value of an estimated standard deviation (k = 1).

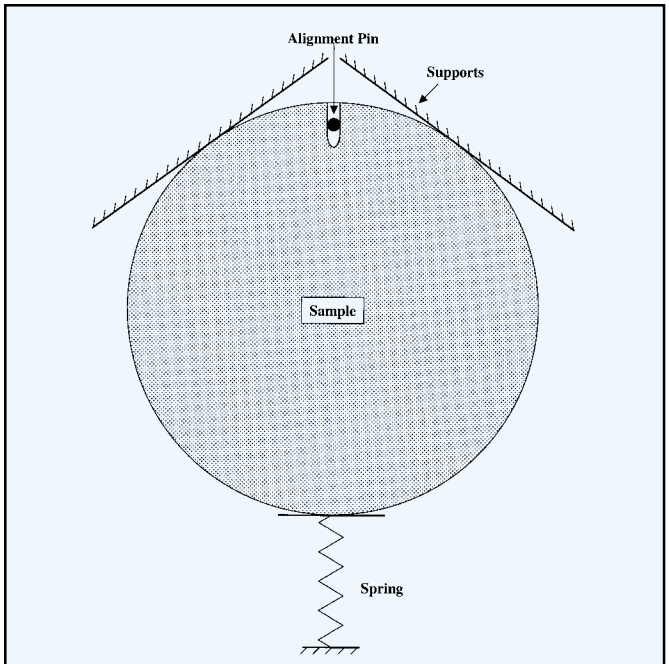

Figure 3—Schematic illustration of a coating sample held in place by the specially fabricated sample holder, which is used to place the sample on the AFM stage in a particular orientation.

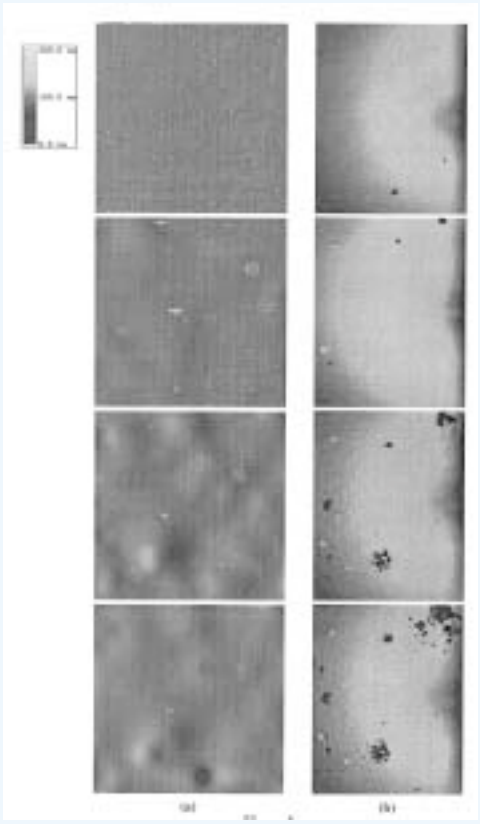

Figure 4—(a) AFM images and (b) corresponding optical images of the acrylic melamine coating after exposure to 50°C, 70% RH, and no UV radiation for (from top to bottom) 0, 6, 27, and 53 days. For all AFM images, lateral dimensions are 100 µm × 100 µm, and the height scale from white to black corresponds to 200 nm. Optical images have approximate dimensions of 675 µm × 530 µm.

dation chemistry has been studied extensively.[5,6] The acrylic melamine coating was made from a mixture of a hydroxy-functional acrylic polymer and a partially alkylated amino crosslinking agent at a mass ratio of 70:30. The acrylic polymer (DuPont) contained by mass 58% n-butylmethacrylate, 40% hydroxy ethylacrylate, and 2% acrylic acid and was supplied as a mixture by mass of 75% acrylic polymer and 25% 2-heptanone. The amino crosslinking agent was Cymel 325 (Cytec), which is a mixture containing by mass 80% melamine formaldehyde resin and 20% isobutanol solvent. No pigments were used in the coating formulation. The proposed structure for the cured coating system is shown in *Figure* 2 and is based on evidence from FTIR spectroscopy.

Coatings were applied to calcium fluoride disks using a spin-coating technique. The calcium fluoride disks were 100 mm in diameter and 9 mm in thickness. Calcium fluoride was chosen as the substrate because it has excellent moisture and heat resistance properties and is transparent to both UV and infrared radiation,[14] allowing for periodic characterization of spectral UV-visible and infrared transmittance. For each coating system, the chemical components were mixed in the appropriate ratio, degassed, spread onto the substrate, and spun cast at 21 rad/sec (200 revolutions per minute) for 30 sec. The acrylic melamine samples were cured at 130°C for 20 min, and complete cure was verified using FTIR spectroscopy. Also using FTIR spectroscopy, the average coating thickness was estimated to be 11.4 µm ± 0.5 µm.

The geometry of a coating sample is shown in *Figure* 1, and the regions of the sample that were monitored are indicated by the dashed circles. For example, the windows along the perimeter were utilized to expose areas of the coating to the specific UV wavelengths discussed in the previous section (290, 294, 300, etc., up to 450 nm) as indicated in *Figure* 1. The center position and the 12th position were exposed to the "full" UV spectrum emitted by the solar simulators and no UV radiation, respectively.

A full-factorial experimental design, as detailed elsewhere,[3] for the acrylic melamine samples was employed: samples were exposed to a range of relative humidities (less than one percent RH up to 90% RH), different temperatures (30, 40, 50, and 60°C), and different UV wavelengths (or no UV exposure). One replicate was used in each treatment. The samples were periodically removed from the exposure apparatus and analyzed using UV-visible spectrometry, FTIR-transmission spectroscopy, and AFM. Analyses of spectral UV-visible measurements and FTIR spectra were made at the center points of each of the exposure areas on all exposed samples each time they were removed, the results of which are detailed elsewhere.[3] Additionally, the spatial and spectral radiant intensities of the light source and the spectral transmittances of the interference filters and the quartz plate were also monitored and recorded at each inspection period.[3] Due to experimental time constraints, AFM analysis was per-

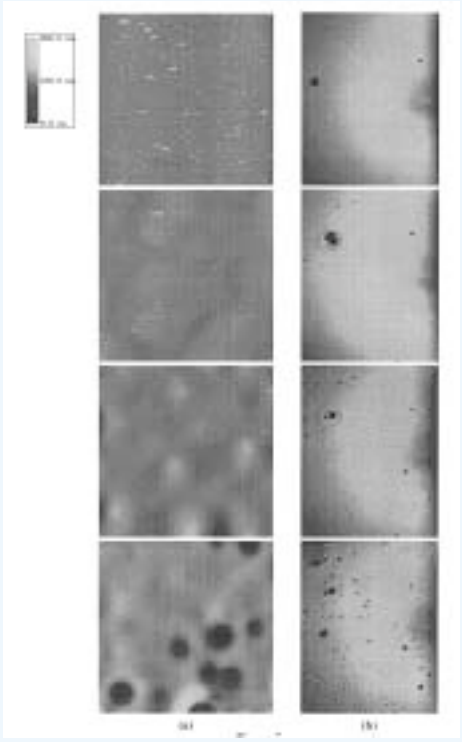

Figure 5—(a) AFM images and (b) corresponding optical images of the acrylic melamine coating after exposure to 50°C, 70 % RH, and the UV spectrum of the solar simulator for (from top to bottom) 0, 6, 27, and 53 days. For all AFM images, lateral dimensions are 100 µ × 100 µm, and the height scale from white to black corresponds to 200 nm. Optical images have approximate dimensions of 675 µm × 530 µm.

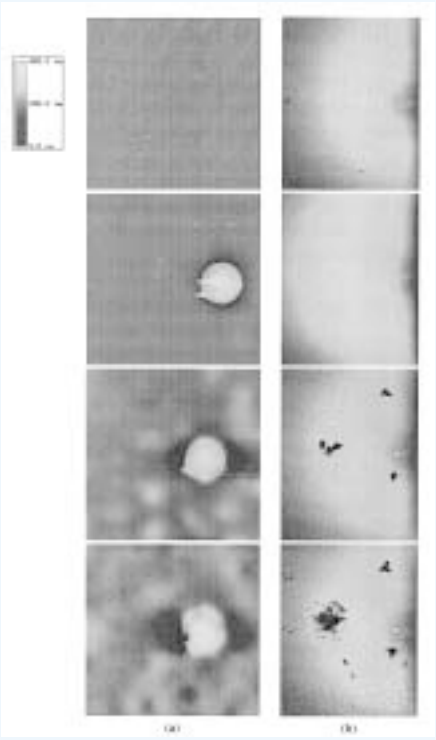

Figure 6—(a) AFM images and (b) corresponding optical images of the acrylic melamine coating after exposure to 50°C, 70% RH, and 326 nm UV radiation for (from top to bottom) 0, 6, 27, and 53 days. For all AFM images, lateral dimensions are 100 µm × 100 µm, and the height scale from white to black corresponds to 400 nm. Optical images have approximate dimensions of 675 µm × 530 µm.

formed on a small sample set. Several regions of the sample exposed to 50°C and 70% RH were monitored for exposure times of up to 1270 hr (53 days). These regions were those exposed to the full UV spectrum output of the light source, no UV radiation, radiation at 294 nm, and radiation at 326 nm. Within each of these exposed regions, three areas were sampled to better assess the uniformity of damage to the specimen. For brevity, only results for "full" UV, no UV, and 326 nm radiation will be presented.

Atomic Force Microscopy

In AFM, a probe consisting of a sharp tip (nominal tip radius on the order of 10 nm) located near the end of a cantilever beam is raster-scanned across the sample surface using piezoelectric scanners. Changes in the tip-sample interaction are normally monitored using an optical lever detection system, in which a laser beam is reflected off the cantilever and onto a position-sensitive photodiode. In this study, tapping mode images of 100 µm × 100 µm regions were constructed. In tapping mode, the cantilever oscillates close to its first bending mode resonance frequency (normally on the order of 100 kHz) so that the tip makes contact with the sample only for a short duration in each oscillation cycle. As the tip approaches the sample, the tip-sample interactions alter the amplitude, resonance frequency, and phase angle of the oscillating cantilever. During scanning, the amplitude at the operating frequency is maintained at a constant level, called the set-point amplitude, by adjusting the relative position of the tip with respect to the sample. Images are generated through a feedback loop between the optical detection system and the piezoelectric scanners.

To image the coating samples, a Dimension 3100 AFM (Digital Instruments) was used. A special sample holder was fabricated into which a circular coating sample could be repeatedly placed in the same orientation and secured (see *Figure* 3). To monitor the same region of the specimen, a small x-shaped reference mark that was scribed into the coating was located with the AFM's integrated optical microscope and precision x-y stage and centered in the crosshairs of the video display. The x-y coordinates were reset to (0,0) to set the reference mark as the new origin of the x-y stage. The coordinates of each area to be scanned, which were determined during scanning of the as-processed coatings, could then be entered to position the same region under the AFM probe precisely and consistently. As a check, reference marks were made within the areas viewed with the optical microscope but well away from the region to be imaged. The AFM's video capture system was used to check the alignment of each reference

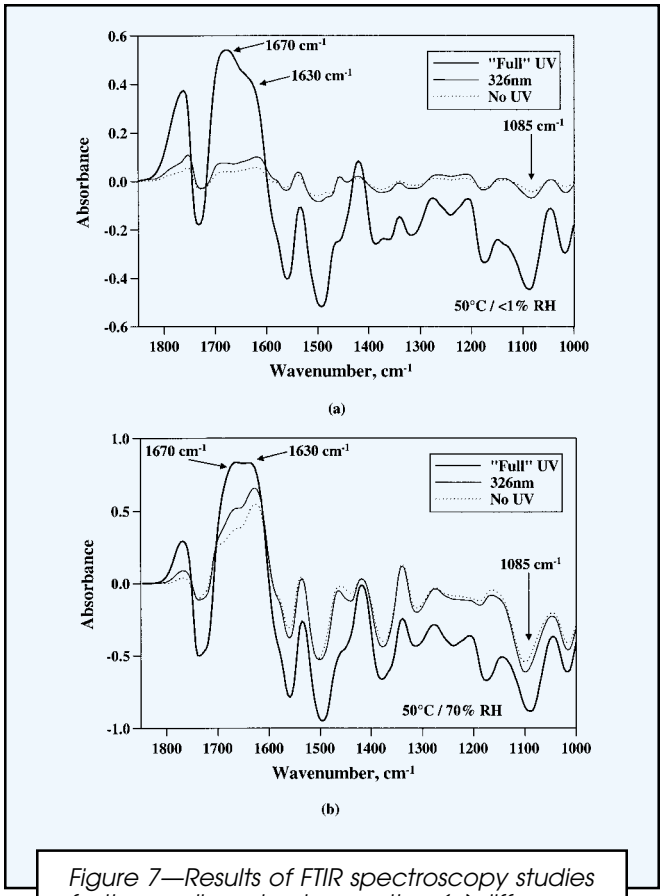

Figure 7—Results of FTIR spectroscopy studies for the acrylic melamine coating: (a) difference spectra after exposure to 50°C, 70% RH for different levels of UV exposure; (b) difference spectra after exposure to 50°C, less than one percent RH for different levels of UV exposure.

mark prior to scanning the corresponding region of interest. In some cases, slight manual adjustments in the sample position were made prior to scanning.

RESULTS

AFM scans of acrylic melamine samples were performed in the center regions of the areas exposed to 50°C and 70% RH and various UV conditions: one area was not exposed to UV radiation; one was exposed to the full spectrum emitted by the light source (no cut-off filter was used); and one was exposed to 326 nm UV radiation. Examples of the observed degradation for these areas are shown in *Figures* 4, 5, and 6, respectively. In these figures, a set of AFM images is shown for a single area prior to exposure and after exposure times of 6, 27, and 53 days. The corresponding optical images are also shown.

In all of the AFM images of the as-processed coating, small protuberances were observed that might be defects caused by the high solvent evaporation rates involved in the spin coating process. Many of these bumps disappeared within the first six days of exposure and after 27 days of exposure, little evidence of these bumps remained. Also within the first six days of exposure, several bright,

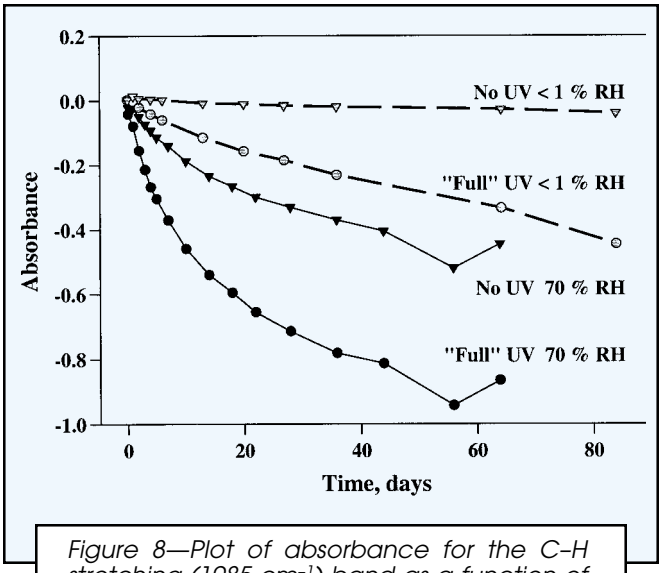

Figure 8—Plot of absorbance for the C–H stretching (1085 cm^{-1}) band as a function of exposure time for exposure to the "full" UV spectrum and to no UV radiation under both 70% RH and less than one percent RH.

circular features were observed in many of the optical images (see, for example, *Figures* 4 and 6). Several of these features formed in the areas scanned with the AFM, one example of which is shown in *Figure* 6. These new protuberances appear to have formed on the surface early in the exposure experiments and do not appear to change significantly with increasing exposure time. In addition, the surface roughness increased over the first 27 days of exposure, during which topographically depressed areas formed and became pits between 27 and 53 days of exposure. These results will be discussed further with respect to the FTIR spectroscopy data in the following section.

DISCUSSION

Exposure of unpigmented acrylic melamine coatings to 50°C and 70% RH caused significant physical and chemical degradation. To correlate physical changes observed using AFM to chemical degradation, FTIR spectroscopy was used in transmission mode to monitor certain infrared bands and estimate the average degradation through the coating thickness from changes in those bands. Results from FTIR-transmission spectroscopy are shown in *Figures* 7 and 8. Difference spectra are shown for a wavelength region of 1000 cm^{-1} to 1850 cm^{-1} for samples exposed to dry (less than one percent RH) and humid (70% RH) conditions in *Figures* 7a and 7b, respectively. These spectra correspond to 63 days of exposure and are shown for the regions of the coating exposed to the "full" UV spectrum of the solar simulator, 326 nm UV radiation, and no UV radiation. Positive absorbance corresponds to formation of reaction products and negative absorbance corresponds to depletion of reacting species. As discussed in detail elsewhere,[15,16] the most important bands related to the degradation of acrylic melamine are the bands at 1670 cm^{-1}, 1630 cm^{-1}, and 1085 cm^{-1}. The 1670 cm^{-1} and 1630 cm^{-1} bands are related to the formation of amide groups

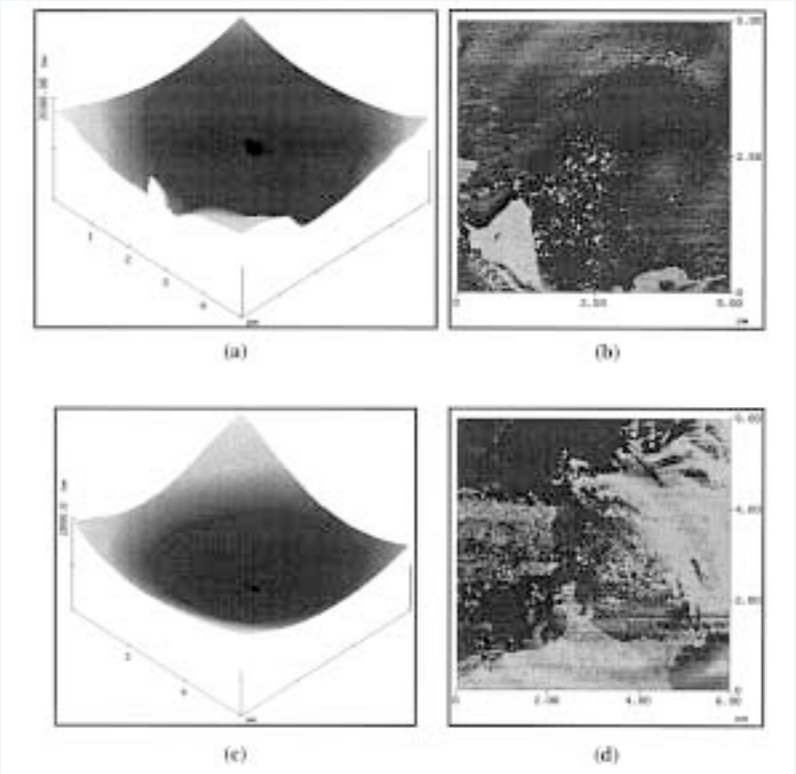

Figure 9—High-resolution AFM images of two different pits in an acrylic melamine sample, with three-dimensional representations of topography in (a) and (c), respectively, and corresponding phase images in (b) and (d), respectively. The color scale from white to black for each topographic image corresponds to a height difference of two μm, whereas that for the phase images corresponds to a phase difference of 90°.

during both photolysis and hydrolysis degradation reactions, while the 1630 cm^{-1} band is also related to the formation of amine groups during photolysis. The decrease in absorbance for the 1085 cm^{-1} band is an indication of chain scission in acrylic melamine and is shown in *Figure* 8 for regions of the coating exposed to the "full" UV spectrum and to no UV radiation under both dry and humid conditions.

From the FTIR results, this acrylic melamine coating appears to undergo significant hydrolysis when exposed to 70% RH. This conclusion, based on the results of a full-factorial experimental program, is evident in the results of *Figure* 8. Essentially, the difference in the absorbance between samples exposed to the no UV, dry environment and those exposed to the "full" UV, dry environment is an indication of photolytic damage. However, the difference in absorbance between samples exposed to the no UV, dry environment and those exposed to the no UV, 70% RH environment is an indication of hydrolytic damage. Thus, hydrolysis appears to play a large role in the degradation of acrylic melamine. Also, as observed in *Figure* 7, the absorbances at 1670 cm^{-1} and 1630 cm^{-1} are greater for exposure to no UV and 70% RH compared to exposure to "full UV" and less than one percent RH. The combination of exposure to "full" UV radiation and 70% RH causes the most degradation, as hydrolysis and photolysis reactions both occur along with moisture-enhanced photolysis.[16]

The formation of bright, circular protuberances on the surface of the coating was observed in both the optical (see *Figures* 4 and 6) and AFM images (see *Figure* 6) for samples exposed to 70% RH. These features might be related to the formation of hydrolysis products, such as those related to the 1670 cm^{-1} and 1630 cm^{-1} bands (see *Figure* 7). Other physical degradation in the form of pits with lateral dimensions from tens of nanometers to several micrometers was also observed, particularly after 53 days of exposure (see *Figures* 4 and 5). The depths of these pits increased with exposure time, such that they grew through the coating. The cause of the formation of these localized pits is unknown. One explanation could be related to the similarity of these microscopic pits to macroscopic pits that form as a result of material loss due to acid catalyzed hydrolysis often referred to as environmental or acid etching.[17-19] Acid catalyzed hydrolysis results in the chain scission process at the ether linkages that has been monitored using the 1085 cm^{-1}. Instead of coming from the environment, however, acid that is present in the coating formulation[20] (two percent by mass of acrylic acid was used in the present study) as well as acid generated by reactions of formaldehyde and oxygen (O_2)[16] can catalyze hydrolysis-related chain scission reactions during exposure of acrylic melamine to humid environments. Because this chemistry occurs locally at the molecular level rather than over a region covered by a water droplet, the resulting pits are of a much smaller size than those observed in environmental etching situations.

In general, pits were observed after 27 to 53 days of exposure, and within the limited number of local regions imaged with the AFM, pits that formed during this time period grew in depth and in breadth often without new pits forming as exposure time increased. This observation would suggest an autocatalytic process, which would be consistent with an acid-catalyzed hydrolysis process. Another potential autocatalytic process that would explain our observations is as follows. The pits originate from defects in the coating that are particularly susceptible to either UV radiation or moisture or both. At these defect points, crosslinks are broken through the absorbance of UV radiation by chromophores that are distributed throughout the coating. When a chromophore absorbs radiation, it can form radicals that react with network molecules in close proximity to break crosslinks and create new chromophores, thus renewing the process within the same local region.

Another explanation could be that the chemical degradation process is essentially a reversal of the curing process, for which the extent of reaction increases (mass fraction of sol decreases) rapidly upon gelation and then

slows dramatically at high percentage conversion. During degradation, the mass fraction of sol would be very low until significant degradation had occurred, at which point the physical consequences of this degradation might be observed, i.e., in the form of pits. Also, the presence of moisture might enhance the occurrence of physical degradation by providing a transport process that allows sol to move away from degraded areas, leaving behind pits in the surface.

In any case, once the chemical degradation of various local regions has progressed such that numerous pits and other surface defects have formed, these defects could become critical flaws, particularly if the coating embrittles during the same exposure period. These critical flaws could then propagate through the thickness of the coating due to internal stresses, such as those induced by temperature or moisture content fluctuations.[21] A catastrophic change in coating appearance and performance could be produced as a result of such cracking, as has been observed for automotive clearcoats in service.[7]

These ideas pertaining to the formation of pits and their effects on coating failure are purely speculative at this time. More extensive research is needed to understand the relationships between chemical and physical degradation of polymer coatings. Note, however, that a more complete study of physical degradation will require use of optical methods in addition to AFM to evaluate larger scale topological changes due to the limitations of the AFM for imaging areas larger than 100 µm x 100 µm. Further, to provide statistically relevant information about the relative topological changes due to the different exposure conditions, statistical random sampling of the surfaces should be used. Such an extensive investigation was not performed in this initial work, and thus *Figures* 4-6 do not provide an adequate basis for comparing the relative amounts of physical damage caused by the different exposure environments.

Using higher resolution AFM imaging to study 5 to 6 µm square areas of the degraded samples, heterogeneity was observed in the pits of the acrylic melamine coating, as shown in the phase contrast images of *Figure* 9, i.e., *Figures* 9b and 9d. The corresponding topography of the pits is shown in three-dimensional form in *Figures* 9a and 9c, respectively. No such heterogeneity was observed in similar images taken in regions where no pitting was observed (not shown). Therefore, the presence of the observed heterogeneity may be related to the sensitivity of acrylic melamine to moist environments. Further studies are needed to establish whether the coating is initially heterogeneous or whether the heterogeneity is created during degradation. If the latter explanation is true, then the origin and characteristics of this heterogeneity will need to be established in order to assess its effect on further degradation.

SUMMARY

The atomic force microscope (AFM) was used to monitor changes in surface features of an acrylic melamine coating that was exposed to a variety of weathering conditions. A technique was developed such that, upon periodic removal from the weathering environment, the same 100 µm ´ 100 µm regions of the samples could be scanned. The acrylic melamine coating was very sensitive to moist environments, degrading more rapidly and to a larger extent under conditions of high relative humidity compared to very dry conditions, as observed using FTIR spectroscopy. Significant physical degradation, which included a general roughening of the surface, the formation of protuberances thought to be related to hydrolysis products, and the formation of pits, was observed for exposure to 70% RH.

A mechanism for the formation of pits in the surface is postulated based on known mechanisms of chemical degradation of the acrylic melamine polymer. In general, chromophores that are distributed throughout the coating absorb radiation and form radicals that react with network molecules in close proximity to break crosslinks. The chain scission process creates new chromophores, thus renewing the process and causing high degradation rates in these local regions. Also, if the chemical degradation process is essentially a reversal of the curing process, the local mass fraction of sol would be very low until significant degradation had occurred. The presence of moisture might be needed to provide a transport process that allows sol to move away from degraded areas, leaving behind pits in the surface. The microscopic pits could then act as crack tips and grow through the thickness of the coating due to changes in internal stresses, such as those induced by temperature fluctuations or moisture absorption. A catastrophic change in coating appearance and corrosion resistance would result, as has been observed in service exposure conditions. Coating heterogeneity was observed in degraded regions of the acrylic melamine samples and could enhance coating degradation by creating preferential sights for moisture adsorption. These postulated mechanisms are currently under further investigation.

ACKNOWLEDGMENTS

The authors would like to acknowledge the support of the NIST/government/industry consortium on the Service Life Prediction of Organic Coatings. Also, the authors are grateful to Steve Nixon and Dr. Colin Cameron of Akzo Nobel for the helpful conversations regarding photodegradation mechanisms of the coating samples.

References

(1) Climate Research Committee, *Natural Climate Variability on Decade-to-Century Time Scales*, National Academy of Science Press, Washington, DC, 1995.
(2) Martin, J.W., "A Critical Review of the Role of Field Exposure Experiments in Predicting the Service Life of Coatings," *Durability of Coatings on Plastics*, Ryntz, R.A. (Ed.), Hanser, New York, 2000.
(3) Martin, J.W., Nguyen, T., Byrd, E., Dickens, B., and Embree, E., "Relating Laboratory and Outdoor Exposures of Acrylic Melamine Coatings: I. Estimation of Total Absorbed Dosage and Spectral Quantum Yield," *Poly. Degrad. Stab.*, submitted for publication, 2000.
(4) Bauer, D.R., "Melamine/Formaldehyde Crosslinkers: Characterization, Network Formation and Crosslink Degradation," *Prog. Org. Coat.*, 14, No. 3, 193 (1986).

(5) Bauer, D.R., Gerlock, J.L., and Mielewski, D.F., "Photostabilization and Photodegradation in Organic Coatings Containing a Hindered Amine Light Stabilizer.7. HALS Effectiveness in Acrylic Melamine Coatings Having Different Free-Radical Formation Rates," *Poly. Degrad. Stab.*, 36, No. 1, 9 (1992).
(6) Bauer, D.R. and Mielewski, D.F., "The Role of Humidity in the Photooxidation of Acrylic Melamine Coatings," *Poly. Degrad. Stab.*, 40, No. 3, 349 (1993).
(7) Hill, L.W., "Overview of Mechanical Property Changes During Coating Degradation," *Service Life Prediction of Organic Coatings: A Systems Approach*, ACS Symposium Series 722, Bauer, D.R. and Martin, J.W. (Eds.), American Chemical Society, Washington, DC, pp. 312-322, 1999.
(8) Hill, L.W., Korzeniowski, H.M., Ojunga-Andrew, M., and Wilson, R.C., "Accelerated Clearcoat Weathering Studied By Dynamic-Mechanical Analysis," *Prog. Org. Coat.*, 24, No. 1-4, 147 (1994).
(9) Nichols M.E., Gerlock J.L., and Smith C.A., "Rates of Photooxidation Induced Crosslinking and Chain Scission in Thermoset Polymer Coatings," *Poly. Degrad. Stab.*, 56, No. 1, 81 (1997).
(10) Nichols M.E., Darr C.A., Smith C.A., Thouless, M.D., and Fischer, E.R., "Fracture Energy of Automotive Clearcoats – I. Experimental Methods and Mechanics," *Poly. Degrad. Stab.*, 60, No. 2-3, 291 (1998).
(11) Lee, F., Pourdeyhimi, B., and Adamsons, K., "Analysis of Coatings Appearance and Surface Defects Using Digital Image Capture-Processing-Analysis System," *Service Life Prediction of Organic Coatings: A Systems Approach*, ACS Symposium Series 722, Bauer, D.R. and Martin, J.W. (Eds.), American Chemical Society, Washington, DC, pp. 207-232, 1999.
(12) Klein, W.H. and Goldberg, B., "Monitoring UVB Spectral Irradiances at Three Latitudes," *Proc. International Solar Energy Society Conference* (Vol. 1), 400 (1978).
(13) Prane, J.A., "Introduction to Polymers and Resins," *Federation Series on Coatings Technology*, Federation of Societies for Coatings Technology, Philadelphia, PA, 1986.
(14) Rancourt, J.D., *Optical Thin Films User's Handbook*, McGraw-Hill, New York, p, 183, 1987.
(15) Nguyen, T., Martin, J.W., Byrd, E., and Embree, N., "Effects of Relative Humidity on Photodegradation of Acrylic Melamine Coatings: A Quantitative Study," *Proc. American Chemical Society Division of Polymeric Materials: Science and Engineering*, American Chemical Society, Washington, DC, 83, 188 (2000).
(16) Martin, J.W., Nguyen, T., Byrd, E., Dickens, B., and Embree, E., "Relating Laboratory and Outdoor Exposures of Acrylic Melamine Coatings: II. Effects of Relative Humidity on Photodegradation, Absorbed Dosage and Apparent Quantum Yields of Acrylic-Melamine Coatings," JOURNAL OF COATINGS TECHNOLOGY, submitted for publication, 2001.
(17) Gregorovich, B.V. and Hazan, I., "Environmental Etch Performance, and Scratch and Mar of Automotive Clearcoats," *Prog. Org. Coat.*, 24, No. 1-4, 131 (1994).
(18) Holoubka, J.W., Schmitz P.J., and Xu, L.-F., "Acid Etch Resistance of Automotive Clearcoats. I: Laboratory Test Method Development," JOURNAL OF COATINGS TECHNOLOGY, *72*, No. 901, 77 (2000).
(19) Schmitz, P.J., Holoubka, J.W., and Xu, L.-F., "Mechanism for Environmental Etch of Acrylic Melamine-Based Automotive Clearcoats: Identification of Degradation Products," JOURNAL OF COATINGS TECHNOLOGY, *72*, No. 904, 39 (2000).
(20) Bauer, D. R., "Degradation of Organic Coatings. I. Hydrolysis of Melamine Formaldehyde/Acrylic Copolymer Films," *J. Appl. Polym. Sci.*, 27, No. 10, 3651 (1982).
(21) Nichols, M.E. and Darr, C.A., "The Effect of Weathering on the Stress Distribution and Mechanical Performance of Automotive Paint Systems," *Service Life Prediction of Organic Coatings: A Systems Approach*, ACS Symposium Series 722, Bauer, D.R. and Martin, J.W. (Eds.), American Chemical Society, Washington, DC, pp. 332-353, 1999.